



Contents lists available at ScienceDirect

Journal of Organometallic Chemistry

journal homepage: www.elsevier.com/locate/jorganchem

Synthesis, characterization, and reactivity of Cp^{*}Rh(III) complexes having functional N,O chelate ligands

Lloyd Munjanja, Hongmei Yuan, William W. Brennessel, William D. Jones^{*,1}

Department of Chemistry, University of Rochester, Rochester, NY 14627, USA

ARTICLE INFO

Article history:

Received 3 October 2016

Received in revised form

10 February 2017

Accepted 11 February 2017

Available online xxx

Keywords:

Rhodium

Catalysis

Dehydrogenation

Non-innocent ligands

ABSTRACT

Cp^{*}Rh(III) complexes **1a** and **1b** (Cp^{*} = 1, 2, 3, 4, 5-pentamethylcyclopentadienyl) having functional N,O chelate ligands have been synthesized and characterized by ¹H, ¹³C{¹H} NMR spectroscopy, elemental analysis, IR spectroscopy and X-ray diffraction. Reactivity of these complexes has been investigated towards dehydrogenation of alcohols and hydrogenation of ketones. It was found that these compounds are precursors to the formation of Rh nanoparticles which serve as catalysts, as evidenced by mercury poisoning of the catalysis and direct observation of the particles by TEM, EDX, and XRD.

© 2017 Elsevier B.V. All rights reserved.

1. Introduction

With the rise in the need for liquid organic hydrogen storage materials [1], acceptorless alcohol dehydrogenation (AAD) becomes a favorable atom-economical approach for alcohol oxidation [2]. Alcohols and carbohydrates derived from renewable biomass present an opportunity for such materials as they can be oxidized with the concomitant release of hydrogen [3]. In addition, the carbonyl compounds derived from the AAD process can be used for the formation of imines, amides, and esters [4].

A significant number of catalysts have been discovered for this process [5]. Cp^{*}Ir (Cp^{*} = 1,2,3,4,5-pentamethylcyclopentadienyl) catalysts bearing the functional N,O and C,N chelating ancillary ligands first developed by Fujita and co-workers caught our attention as useful catalysts [6a–b]. The Fujita Cp^{*}Ir catalysts with N,O and C,N chelating ligands were efficient for the reversible acceptorless dehydrogenation of alcohols. The origin of the exceptional reactivity of the iridium catalysts Cp^{*}Ir(2-hydroxypyridine)Cl₂, and Cp^{*}Ir[(2-OH-6-phenyl)pyridine]Cl (**Ir-1**, Fig. 1) was demonstrated through the protic functional group on the ligand that promotes the release of dihydrogen from the metal hydride intermediate.

Inspired by the –OH functionality of the Fujita catalysts, our group has developed nickel Tp'-stabilized (Tp': tris(3,5-dimethylpyrazolyl)borate) catalyst incorporating 2-hydroxypyridine [7]. These nickel catalysts with functional N, O ligand were efficient in the acceptorless, reversible dehydrogenation-hydrogenation of alcohols just as their iridium analogs.

Employing the Fujita-Yamaguchi catalyst Cp^{*}Ir[(2-OH-6-phenyl)pyridine]Cl, **Ir-1**, we successfully demonstrated a tandem catalytic process upgrading ethanol to *n*-butanol with up 99% selectivity [8]. No reaction was observed with the unfunctionalized Cp^{*}Ir(2-phenylpyridine)Cl catalyst showing the significant role of hydroxyl (–OH) moiety on the **Ir-1** catalyst in facilitating the dehydrogenation and hydrogenation steps [6]. With the success of the **Ir-1** catalyst in both dehydrogenation of primary and secondary alcohols, we sought to synthesize the analogous rhodium catalyst, **Rh-1** (Fig. 1) with similar hydroxyl (–OH) functionality to explore differences in catalytic reactivity for the dehydrogenation of alcohols.

2. Results and discussion

2.1. Synthesis of Cp^{*}Rh(III) complexes **1a** and **1b**

The attempted synthesis of **Rh-1** following closely the synthetic procedure used for preparation of **Ir-1** was unsuccessful [6b]. The reaction of [Cp^{*}RhCl₂]₂ with 6-phenyl-2-pyridone in the presence of NaOAc in dichloromethane at room temperature exclusively gave

* Corresponding author.

E-mail address: jones@chem.rochester.edu (W.D. Jones).

¹ This article is dedicated to Professor John Gladysz on the occasion of his 65th birthday.

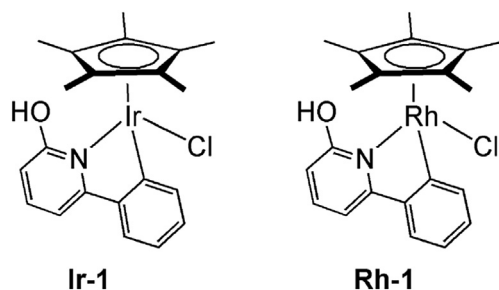
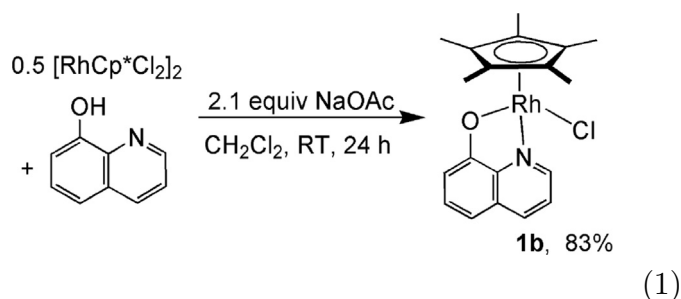


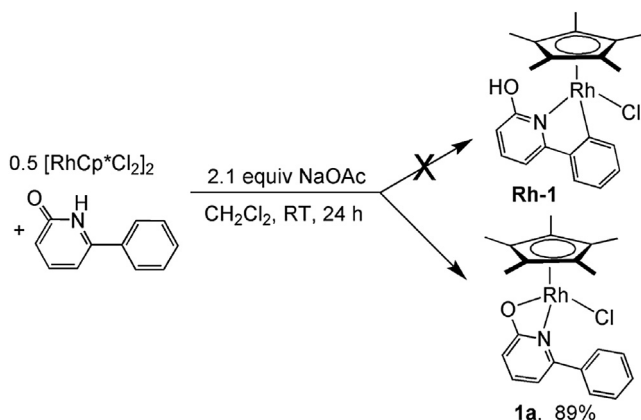
Fig. 1. Known catalyst $\text{Cp}^*\text{Ir}[(2\text{-OH-6-phenyl)pyridine}]\text{Cl}$ **Ir-1** (left [6b]) and proposed catalyst $\text{Cp}^*\text{Rh}[(2\text{-OH-6-phenyl)pyridine}]\text{Cl}$, **Rh-1** (right).

the N,O chelated complex **1a** rather than the anticipated C,N chelated product, **Rh-1** (Scheme 1). Complex **1a** was isolated as a red solid that is stable indefinitely under air and moisture. To our surprise, there has been no reported Cp^*Rh catalyst with N,O chelation.

Employing stronger bases such as PhCO_2Na to promote C–H activation [9] of 6-phenyl-2-pyridone did not give the desired product **Rh-1**. To confirm the preference for N,O chelation a separate experiment was conducted with $[\text{Cp}^*\text{RhCl}_2]_2$ and 8-hydroxyquinoline in the presence of NaOAc in dichloromethane at room temperature. Indeed, complex **1b** was formed with N,O chelation (eq (1)).



Complexes **1a** and **1b** were characterized by ^1H and $^{13}\text{C}\{^1\text{H}\}$ NMR spectroscopy, elemental analysis, and infra-red spectroscopy. The five-membered metallacycle **1b** shows the Cp^* resonance further downfield at δ 1.71 compared to the four membered metallacycle **1a** at δ 1.45 in the ^1H NMR spectrum in CD_2Cl_2 . Neither C=O nor N–H stretches are observed in the solid state IR spectrum.



Scheme 1. Preferential formation of N,O chelation complex **1a** over C,N complex **Rh-1** from the reaction of 6-phenyl-2-pyridone and $[\text{Cp}^*\text{RhCl}_2]_2$.

Single crystals suitable for X-ray diffraction were obtained for **1a** by layering a CH_2Cl_2 solution with pentane. The structure shows a monomeric complex bearing Cp^* and a N,O chelate ligand (Fig. 2). In complex **1a** the carbon–oxygen bond is 1.295(3) Å, a distance in between that expected for a single or double bond. Related N,O chelate complexes of iridium and nickel show this delocalized behavior [6a, 7].

Unfortunately, single crystals for **1b** were challenging to obtain, but addition of an excess of NaOAc to **1b** in CH_2Cl_2 replaced the chloride with an acetate ligand to give **1b'**. Crystals of complex **1b'** were obtained by layering a CH_2Cl_2 in pentane. X-ray diffraction confirms the N,O chelated complex with a monodentate acetate ligand (Fig 3). The N1–Rh–O1 angle for the five membered metallacycle **1b'** is 78.30° , much larger compared to 61.92° for the four membered complex **1a**. The Rh–O bonds are 2.1581 and 2.126 Å for **1a** and **1b'** respectively. In addition, the Rh–N bonds of 2.1357 and 2.090 Å are in the normal range of typical Rh–N bond lengths [10]. Complexes **1a** and **1b'** both adopt a 3-legged piano stool configuration.

2.2. Rhodium vs. iridium selectivity

Davies and coworkers have reported formation of cyclo-metallated rhodium and iridium complexes with various nitrogen donor ligands using NaOAc to deprotonate the C–H bond [11]. Following Davies' synthetic approach, we have reported formation of C,N iridium and rhodium complexes from the reactions of $[\text{Cp}^*\text{MCl}_2]_2$ ($\text{M} = \text{Ir}, \text{Rh}$) and substituted phenyl imines and 2-phenylpyridines [10]. Consequently, it was surprising for the reaction of $[\text{Cp}^*\text{RhCl}_2]_2$ with 6-phenyl-2-pyridone to favor the N,O product **1a** instead of the C,N product, **Rh-1**. DFT calculations employed on the N,O chelated Rh complex **1a** versus **Rh-1** showed that **1a** is 12.6 kcal/mol more thermodynamically preferred than **Rh-1**. Interestingly, the same trend is observed for iridium. The N,O chelation product for iridium, **2a**, is more favored than the C,N chelation product **Ir-1** by 8.1 kcal/mol (Scheme 2). On the basis of these calculations one would expect to form N,O chelation complexes for both iridium and rhodium and disfavor C,N chelation products. However, experimentally, the exclusive formation of **1a** (N,O chelation product) is seen for rhodium and exclusive formation of **Ir-1** (C,N chelation product) is seen for iridium. A plausible explanation for this significant difference in reactivity

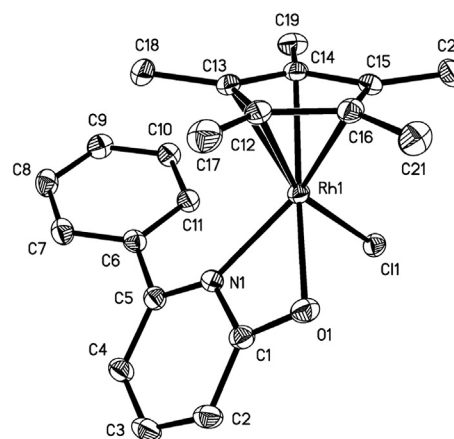


Fig. 2. Thermal ellipsoid drawing of the molecular structure of **1a**. Ellipsoids are shown at the 50% probability level. Selected bond lengths (Å) and angles [$^\circ$]: Rh(1)–O(1) 2.1581(15); Rh(1)–N(1) 2.1357(17); C(1)–O(1) 1.295(3); N(1)–C(1) 1.361(3); N(1)–Rh(1)–O(1); 61.92(6); O(1)–C(1)–N(1) 112.53(18).

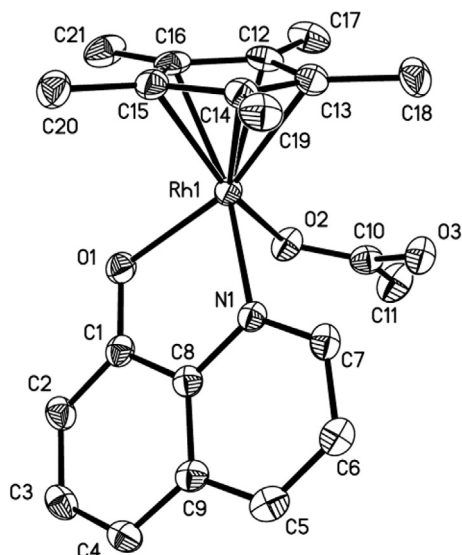
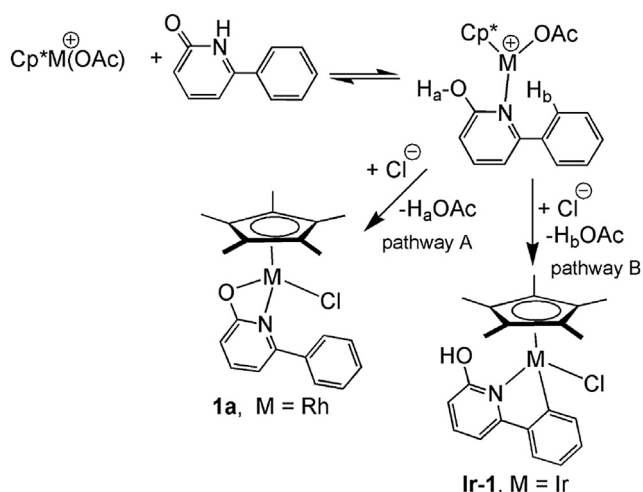


Fig. 3. Thermal ellipsoid drawing of the molecular structure of **1b**. Ellipsoids are shown at the 50% probability level. Selected bond lengths (Å) and angles [°]: Rh(1)–O(1) 2.126(4); Rh(1)–N(1) 2.090(4); C(1)–O(1) 1.323(7); N(1)–C(8) 1.380(6); C(1)–C(8) 1.428(7); N(1)–Rh(1)–O(1) 78.30(15); O(1)–C(1)–C(8) 118.2(5); C(1)–C(8)–N(1) 116.1(4); C(8)–N(1)–Rh(1) 113.7(3).



Scheme 2. Pathway for the preferential formation of N,O chelated Rh complex **1a**.

can be traced back to the differences in electrophilicity of the metal centers, with iridium being the more electrophilic of the two.

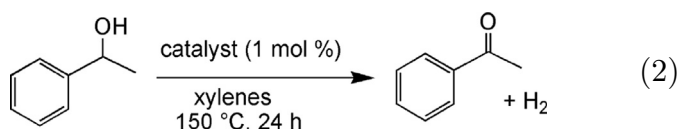
Our group reported that the cationic $[\text{Cp}^*\text{M}(\text{OAc})]^+$ species is responsible for the electrophilic C–H activation of phenylpyridines [10]. $[\text{Cp}^*\text{M}(\text{OAc})]^+$ is generated in situ from the reaction of $[\text{Cp}^*\text{MCl}_2]_2$ and NaOAc. In using 6-phenyl-2-pyridone as the chelating ligand we create two competing pathways for the electrophilic metal centers (Scheme 2). Pathway A involves deprotonation of the acidic phenol proton H_a to yield N,O chelated complexes and pathway B involves C– H_b activation to give C,N chelated complexes. We hypothesize that the exclusive formation of **1a** with the less electrophilic Rh occurs via that the favorable H_a deprotonation (pathway A) by the acetate base to acetic acid rather than C–H activation via H_b . However, in the case of the more electrophilic $[\text{Cp}^*\text{Ir}(\text{OAc})]^+$, interaction with the phenyl π -

system leads to C– H_b activation to give **Ir-1** as the only product (pathway B).

2.3. Catalytic activity of **1a** and **1b**

With the rhodium complexes **1a** and **1b** in hand, the dehydrogenation of 1-phenylethanol to acetophenone with the release of hydrogen was examined. First, the thermal stability of the complexes was investigated by monitoring complex **1a** or **1b** at 150 °C in *p*-xylene by ^1H NMR spectroscopy over 48 h. Approximately 30–40% of complex **1a** slowly decomposed over that time period. In contrast approximately 10% of **1b** decomposed after 48 h. The decomposition products were NMR silent making their identification difficult.

Employing 10 mol% of catalyst **1a**, 1-phenylethanol was heated in toluene- d_8 at 115 °C, resulting in an 80% conversion of 1-phenylethanol to acetophenone (79% yield). Lowering the catalyst loading to 1 mol% of **1a** did not affect the conversion and yield of acetophenone. Changing the solvent to *p*-xylene and heating to 150 °C for 24 h with 1 mol % catalyst **1a** results in 100% conversion of 1-phenylethanol to give 100% yield of acetophenone with the release of hydrogen (eq (2)). In a separate experiment, 1 mol% of **1b** can yield 100% of acetophenone from 1-phenylethanol under similar reaction conditions.



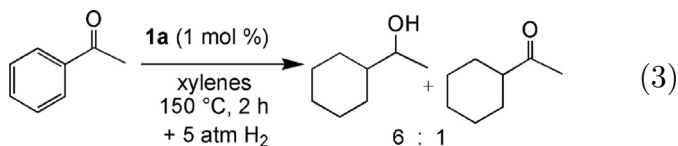
To test the homogeneity of the system we ran the dehydrogenation reaction after the addition of 2 drops of mercury for 24 h with 1 mol% of either **1a** or **1b** in *p*-xylene. For both catalysts we observe a shutdown of the dehydrogenation reaction. Minimal formation of acetophenone is observed in the ^1H NMR spectrum (<10%). To confirm if the reaction was indeed being catalyzed heterogeneously, the formation of acetophenone was monitored over 4 h by ^1H NMR spectroscopy. A plot of the formation of acetophenone over time does not display clean first order kinetics as expected for a homogeneous catalyst (see [Supplementary Information](#)). These observations point to the involvement of nanoparticles.

Additional evidence for nanoparticle formation was obtained by examining the residue left after evaporation of the solution following a dehydrogenation of 1-phenylethanol by TEM. EDX spectroscopy confirmed the presence of rhodium in the particles. The size of the particles was determined by XRD examination of the material, which indicated a ~2 nm diameter (See Supporting Information). Loss of a Cp^* ligand to form an active transfer hydrogenation catalyst has been observed previously [12], and rhodium nanoparticles have recently been reported to dehydrogenate alcohols [13].

These results are quite surprising considering that the reported iridium and nickel N,O complexes appear to be homogenous catalysts in the dehydrogenation of alcohols to carbonyl compounds [6a,7]. Rhodium nanoparticles have been reported previously to facilitate dehydrogenation of ammonia-borane [14]. In addition only a few homogeneous rhodium catalysts can participate in acceptorless dehydrogenation [15,5b], though no rhodium N,O complexes have been reported for dehydrogenation reactions to our knowledge.

Complex **1a** was tested for hydrogenation catalysis. As shown in equation (3), hydrogenation with 5 atm hydrogen at 150 °C leads to a product in which complete hydrogenation of both the ketone and

the aromatic ring has taken place. A small quantity of cyclohexyl methyl ketone is observed, indicating that hydrogenation of the aromatic ring is more facile than hydrogenation of the ketone moiety. This observation is consistent with the known reports that heterogeneous rhodium catalysts can hydrogenate arenes to cyclohexanes [16–19]. Use of 1 atm of H₂ in neat acetophenone produces a 1:1 ratio of these products after 24 h at 150 °C.



3. Experimental section

3.1. General considerations

Unless otherwise noted, all of the organometallic compounds were prepared and handled under a nitrogen atmosphere using standard Schlenk and glovebox techniques. Dry and oxygen-free solvents (CH₂Cl₂, and pentane) were collected from an Innovative Technology PS-MD-6 solvent purification system and used throughout the experiments. Other solvents such as CD₂Cl₂ and CDCl₃ were used as received from commercial sources. ¹H and ¹³C {¹H} NMR spectra were recorded on a Bruker Avance-400 NMR spectrometer. Chemical shift values in ¹H and ¹³C {¹H} NMR spectra were referenced internally to the residual solvent resonances. Infrared spectra were recorded in the solid state on a Thermo Scientific Nicolet 4700 FT-IR spectrometer equipped with smart orbit diamond attenuated total reflectance (ATR) accessory. Elemental analysis was performed by the University of Rochester using a Perkin Elmer 2400 Series II elemental analyzer in CHN mode. TEM images and EDX spectra were recorded on a FEI Tecnai F20 G2 Scanning Transmission Electron Microscope (S)TEM at the URNano Center. XRD data were obtained on a Philips Powder X-ray diffractometer in the Mechanical Engineering X-ray Analysis Laboratory at the University of Rochester.

3.2. Preparation of Cp*RhCl(6-phenylpyridone), **1a**

[Cp*RhCl₂]₂ (50 mg, 0.081 mmol), 6-phenyl-2-pyridone (28 mg, 0.162 mmol), NaOAc (17 mg, 0.207 mmol), and 2 mL of dichloromethane was added to a flame-dried Schlenk flask. The resulting red solution was stirred at room temperature for 24 h after which the solution was filtered through Celite and the filtrate was evaporated under vacuum to obtain a red material. This solid was washed with ~5 mL of pentane and ~1 mL of toluene and dried further in vacuo to afford **1a** (48 mg, 69%). ¹H NMR (500 MHz, CD₂Cl₂): δ 7.92 (d, *J* = 6.9 Hz, 2H, ArH), 7.53–7.34 (m, *J* = 13.5, 7.4 Hz, 4H, ArH), 6.54 (d, *J* = 7.1 Hz, 2H, ArH), 6.06 (d, *J* = 8.5 Hz, 2H, ArH), 1.45 (s, 15H, C₅Me₅); ¹³C {¹H} NMR (126 MHz, CD₂Cl₂): δ 176.81 (CO), 155.63 (ArC), 139.90 (ArC), 129.26 (ArC), 129.25 (ArC), 129.06 (ArC), 92.83 (ArC), 92.77 (ArC), 9.23 (C₅Me₅). Anal. Calcd for C₂₁H₈ClNORh: C, 58.84; H, 1.88; N, 3.27. Found: C, 59.20; H, 1.73; N, 3.01.

3.3. Preparation of Cp*RhCl(8-hydroxyquinoline), **1b**

[Cp*RhCl₂]₂ (200 mg, 0.324 mmol), 8-hydroxyquinoline (94 mg, 0.647 mmol), NaOAc (68 mg, 0.828 mmol), and 10 mL of dichloromethane was added to a flame-dried Schlenk flask. The resulting red solution was stirred at room temperature for 24 h after which the solution was filtered through Celite. The filtrate was

evaporated under vacuum to obtain a red material. This solid was washed with ~15 mL of pentane and dried further in vacuo to afford the **1b** (110 mg, 81%). ¹H NMR (400 MHz, CD₂Cl₂): δ 8.55 (d, *J* = 4.7 Hz, 1H), 8.11 (d, *J* = 8.4 Hz, 1H), 7.39 (dd, *J* = 8.3, 4.8 Hz, 1H), 7.33 (t, *J* = 8.0 Hz, 1H), 6.86 (d, *J* = 7.9 Hz, 1H), 6.81 (d, *J* = 7.4 Hz, 1H), 1.71 (s, 15H). ¹³C {¹H} NMR (126 MHz, CD₂Cl₂): δ 167.76 (s), 146.87 (s), 145.68 (s), 138.13 (s), 131.22 (s), 130.82 (s), 122.69 (s), 114.86 (s), 93.88 (s), 93.81 (s), 9.14 (s). Anal. Calcd for C₁₉H₂₁ClNORh: C, 54.63; H, 5.07; N, 3.35. Found: C, 53.61; H, 5.13; N, 3.15.

3.4. Dehydrogenation of 1-phenylethanol to acetophenone

Complex **1a** or **1b** (26 μmol) and 1-phenylethanol (2.6 mmol, 326 μL) were mixed with 0.5 mL of *p*-xylene in a 3 mL flame-dried ampoule. The solution color was light orange. The ampoule was sealed and stirred at 150 °C for 24 h. After the reaction, the solution was cooled to room temperature, filtered through a short silica gel column, and eluted with diethyl ether (0.3 mL). The resulting filtrate was evaporated under vacuum to afford an oily residue. The ¹H NMR spectrum in CDCl₃ of the product showed acetophenone as the only product. Dehydrogenation of 1-phenylethanol (1 mol % catalyst **1a** or **1b**) in the presence of 2 drops of elemental mercury shut down catalytic activity.

3.5. Hydrogenation of acetophenone at 1 atm and 5 atm H₂

Complex **1a** (42.8 μmol) and acetophenone (4.28 mmol, 500 μL) were mixed in a 500 mL round bottom flask. The sample was placed under 1 atm H₂ heated at 150 °C for ~24 h. After the reaction, the solution was cooled to room temperature. The mixture was filtered through Celite in a glass pipette, and the filtrate diluted with THF. Examination of the product by GC showed the complete disappearance of acetophenone and the appearance of both cyclohexyl methyl ketone and 1-cyclohexylethanol in a 1:1 ratio.

Complex **1a** (12.8 μmol) and acetophenone (1.28 mmol, 150 μL) were mixed with 0.25 mL of *p*-xylene in a Teflon-lined Parr bomb reactor (50 mL). The sample was placed under 5 atm H₂ and heated at 150 °C for ~2 h. After the reaction, the solution was cooled to room temperature and the reactor vented. The mixture was filtered through Celite in a glass pipette, and the filtrate diluted with THF. Examination of the product by GC showed the complete disappearance of acetophenone and the appearance of both cyclohexyl methyl ketone and 1-cyclohexylethanol in a 6:1 ratio.

4. Conclusions

In summary, we have demonstrated the synthesis of N,O chelated Rh complexes **1a** and **1b**. The catalysts decompose upon heating to give nanoparticles, which in turn can efficiently dehydrogenate 1-phenylethanol to give 100% yield of acetophenone with the release of hydrogen. However, hydrogenation of acetophenone leads to both cyclohexyl methyl ketone and 1-cyclohexylethanol. The involvement of rhodium nanoparticles was indicated by inhibition using elemental mercury and direct observation using TEM.

Acknowledgments

Support for this work was provided by the National Science Foundation grant CHE-1360985. L.M and H. Y would like to thank Dr. Sarina Bellows for the computational calculations and insightful discussions.

Appendix A. Supplementary data

X-ray crystallographic data for **1a** and **1b'** are included. CIF files giving crystallographic information, including data collection parameters, bond lengths, fractional atomic coordinates, and anisotropic thermal parameters, for complexes **1a** and **1b'** have been deposited with the CCDC (1503278–1503279) and NMR spectra for the complexes. GC traces for the hydrogenations are shown. TEM, EDX, and XRD data for the nanoparticles.

Supplementary data related to this article can be found at <http://dx.doi.org/10.1016/j.jorganchem.2017.02.015>.

References

- [1] M. Yadav, Q. Xu, *Energy Environ. Sci.* 5 (2012) 9698–9725.
- [2] (a) G. Guillena, D.J. Ramón, M. Yus, *Chem. Rev.* 110 (2010) 1611–1641; (b) C. Gunanathan, D. Milstein, *Science* 341 (2013) 1229712.
- [3] (a) T.C. Jonson, D.J. Morris, M. Wills, *Chem. Soc. Rev.* 39 (2010) 81–88; (b) M. Nielsen, A. Kammer, D. Cozzula, H. Junge, S. Gladiali, M. Beller, *Angew. Chem. Int. Ed.* 50 (2011) 9593–9597; (c) M. Trincado, D. Banerjee, H. Grützmacher, *Energy Environ. Sci.* 7 (2014) 2464–2503.
- [4] (a) G.E. Dobreiner, R.H. Crabtree, *Chem. Rev.* 110 (2009) 681–703; (b) M.A. Esteruelas, N. Honczek, M. Oliván, E. Oñate, M. Valencia, *Organometallics* 30 (2011) 2468–2471; (c) A. Maggi, R. Madsen, *Organometallics* 31 (2012) 451–455; (d) J.W. Rigoli, S.A. Moyer, S.D. Pearce, J.M. Schomaker, *Org. Biomol. Chem.* 20 (2012) 1746–1749; (e) E. Kossoy, Y. Diskin-Posner, G. Leitus, D. Milstein, *Adv. Synth. Catal.* 354 (2012) 497–504; (f) A. Mukherjee, A.S. Nerush, G. Leitus, L.J.W. Shimon, Y.B. David, N.A.E. Jalapa, D. Milstein, *J. Am. Chem. Soc.* 138 (2016) 4298–4301.
- [5] (a) I. Dutta, A. Sarbajna, P. Pandey, S.M.W. Rahaman, K. Singh, J.K. Bera, *Organometallics* 35 (2016) 1505–1513; (b) G. Zeng, S. Sakaki, K.-I. Fujita, H. Sano, R. Yamaguchi, *ACS Catal.* 4 (2014) 1010–1020; (c) T. Zweifel, J.V. Naubron, H. Grützmacher, *Angew. Chem. Int. Ed.* 48 (2009) 559–563; (d) I. Mena, M.A. Casado, V. Polo, P. Garcia-Orduña, F.J. Lahoz, L.A. Oro, *Angew. Chem. Int. Ed.* 51 (2012) 8259–8263; (e) M. Bertoli, A. Choualeb, A.J. Lough, B. Moore, D. Spasyuk, D.G. Gusev, *Organometallics* 30 (2011) 3479–3482.
- [6] (a) K.-I. Fujita, N. Tanino, R. Yamaguchi, *Org. Lett.* 9 (2007) 109–111; (b) K.-I. Fujita, T. Yoshida, Y. Imori, R. Yamaguchi, *Org. Lett.* 13 (2011) 2278–2281; (c) R. Kawahara, K.-I. Fujita, R. Yamaguchi, *J. Am. Chem. Soc.* 134 (2012) 3643–3646; (d) R. Kawahara, K.-I. Fujita, R. Yamaguchi, *Angew. Chem. Int. Ed.* 51 (2012) 12790–12794; (e) G. Zeng, S. Sakaki, K.-I. Fujita, H. Sano, R. Yamaguchi, *ACS Catal.* 4 (2014) 1010–1020.
- [7] S. Chakraborty, P.E. Piszal, C.E. Hayes, R.T. Baker, E.D. Jones, *Organometallics* 34 (2015) 5203–5206.
- [8] S. Chakraborty, P.E. Piszal, C.E. Hayes, R.T. Baker, W.D. Jones, *J. Am. Chem. Soc.* 137 (2015) 14264–14267.
- [9] A.P. Walsh, W.D. Jones, *Organometallics* 34 (2015) 3400–3407.
- [10] L. Li, W.W. Brennessel, W.D. Jones, *Organometallics* 28 (2009) 3492–3500.
- [11] (a) D.L. Davies, O. Al-Duaij, J. Fawcett, M. Giardiello, S.T. Hilton, D.R. Russell, *Dalton Trans.* (2003) 4132–4138; (b) D.L. Davies, S.M.A. Donald, O. Al-Duaij, J. Fawcett, C. Little, S.A. Macgregor, *Organometallics* 25 (2006) 5976; (c) A.J. Davenport, D.L. Davies, J. Fawcett, D.R. Russell, *J. Organomet. Chem.* 691 (2006) 2221–2227; (d) D.L. Davies, S.M.A. Donald, O. Al-Duaij, S.A. Macgregor, M. Polleth, *J. Am. Chem. Soc.* 128 (2006) 4210–4211.
- [12] J. Campos, U. Hintermair, T.P. Brewster, M.K. Takase, R.H. Crabtree, *ACS Catal.* 4 (2014) 973–985.
- [13] L. Yao, J. Zhao, J.-M. Lee, *ACS Sustain. Chem. Eng.* (2017), <http://dx.doi.org/10.1021/acssuschemeng.6b02994>.
- [14] T. Ayvalı, M. Zahmakıran, S. Özkır, *Dalton Trans.* 40 (2011) 3584–3591.
- [15] D. Morton, D.J. Cole-Hamilton, *J. Chem. Soc. Chem. Commun.* (1987) 248–249.
- [16] M. Ohde, H. Ohde, C.M. Wai, *Chem. Commun.* (2002) 2388–2389.
- [17] A. Sánchez, M. Fang, A. Ahmed, R.A. Sanchez-Delgado, *Appl. Catal. A General* 477 (2014) 117–124.
- [18] H. Yang, H. Gao, R.J. Angelici, *Organometallics* 19 (2000) 622–629.
- [19] P. Barbaro, C. Bianchini, V. Dal Santo, A. Meli, S. Moneti, R. Psaro, A. Scaffidi, L. Sordelli, F. Vizza, *J. Am. Chem. Soc.* 128 (2006) 7065–7076.